Title

Impaired calcium sensing distinguishes primary hyperparathyroidism (PHPT) patients with low bone mineral density

Authors

Weber, Thomas J
Koh, James
Thomas, Samantha M
et al.

Publication Date

2017-09-01

DOI

10.1016/j.metabol.2017.06.004

Peer reviewed

HHS Public Access

Author manuscript

Metabolism. Author manuscript; available in PMC 2018 September 01.

Published in final edited form as:

Metabolism. 2017 September ; 74: 22–31. doi:10.1016/j.metabol.2017.06.004.

Impaired calcium sensing distinguishes primary hyperparathyroidism (PHPT) patients with low bone mineral density

Thomas J. Weber, MD[*,1], **James Koh, PhD**[*,2,4], **Samantha M. Thomas, MS**[3,4], **Joyce A. Hogue, BS**[2], **Randall P. Scheri, MD**[2], **Sanziana A. Roman, MD**[2], and **Julie A. Sosa, MD, MA**[1,2,4,5]

[1]Dept. of Medicine, Duke University Medical Center, Durham, NC

[2]Dept. of Surgery, Duke University Medical Center, Durham, NC

[3]Dept. of Biostatistics and Bioinformatics, Duke University

[4]Duke Cancer Institute, Duke University Medical Center

[5]Duke Clinical Research Institute, Duke University Medical Center

Abstract

Context—A subset of PHPT patients exhibit a more severe disease phenotype characterized by bone loss, fractures, recurrent nephrolithiasis, and other dysfunctions, but the underlying reasons for this disparity in clinical presentation remain unknown.

Objective—We sought to identify new mechanistic indices that could inform more personalized management of PHPT.

Design—Pre-, peri-, and postoperative data and demographic, clinical, and pathological information from patients undergoing parathyroidectomy for PHPT were collected. Univariate and partial Spearman correlation was used to estimate the association of parathyroid tumor calcium sensing capacity with select variables.

Patients or Other Participants—An unselected series of 237 patients aged >18 years and undergoing parathyroidectomy for PHPT were enrolled.

Main outcome measures—Calcium sensing capacity, expressed as the concentration required for half-maximal biochemical response (EC50), was evaluated in parathyroid tumors from an unselected series of 74 patients and assessed for association with clinical parameters. The

Corresponding author and person to whom reprint requests should be addressed: Thomas J. Weber, MD, Department of Medicine, Duke University Medical Center, Durham, NC 27710, Phone: 919-668-1367, FAX: 919-668-1366, thomas.weber2@duke.edu.
*These authors contributed equally to the work.

Disclosure statement: TJW, JK, SMT, JAH, RPS, and SAR have nothing to disclose. JAS is a member of the Data Monitoring Committee of the Medullary Thyroid Cancer Consortium Registry supported by GlaxoSmithKline, NovoNordisk, Astra Zeneca, and Eli Lilly.

hypothesis was that greater disease severity would be associated with attenuated calcium sensitivity and biochemically autonomous parathyroid tumor behavior.

Results—Parathyroid tumors segregated into two distinct groups of calcium responsiveness (EC50 <3.0 and ≥3.0 mM). The low EC50 group (n=27) demonstrated a mean calcium EC50 value of 2.49 mM [95% confidence interval (CI): 2.43–2.54 mM], consistent with reference normal activity. In contrast, the high EC50 group (n=47) displayed attenuated calcium sensitivity with a mean EC50 value of 3.48 mM [95% CI: 3.41–3.55 mM]. Retrospective analysis of the clinical registry data suggested that high calcium EC50 patients presented with a more significant preoperative bone mineral density (BMD) deficit with a T-score of −2.7, (95% CI: −3.4 to −1.9) versus 0.9, (95% CI: −2.1 to −0.4) in low EC50 patients ($p < 0.001$). After adjusting for gender, age, BMI, 25 OH vitamin D level and preoperative iPTH, lowest T-score and calcium EC50 were inversely correlated, with a partial Spearman correlation coefficient of −0.35 ($p=0.02$).

Conclusions—Impaired calcium sensing in parathyroid tumors is selectively observed in a subset of patients with more severe bone mineral density deficit. Assessment of parathyroid tumor biochemical behavior may be a useful predictor of disease severity as measured by bone mineral density in patients with PHPT.

Keywords

Primary hyperparathyroidism; parathyroid tumors; calcium sensing; bone mineral density

1.1 Introduction

Primary hyperparathyroidism (PHPT) is a common endocrine neoplastic disorder of calcium metabolism that occurs in 11 to 30 individuals per 100,000 in the U.S. [1]. Since PHPT disproportionately affects the elderly, this overall incidence is likely to rise as the nation's median population ages [2–4]. The prevalence rate among older women aged 65 to 74 years, a cohort already at elevated risk for disabling bone disease, is currently 99 per 100,000 [1, 4]. The disorder can have broad pathophysiologic effects, including nephrolithiasis, neurologic symptoms, and reduced bone density [2, 5]. Incident fractures that occur in the axial (spine) and appendicular (hip/distal forearm) bone are a major source of morbidity in patients with PHPT. Reduced bone mineral density (BMD), the single best predictor of incident fractures and a primary indication for surgical referral, is inversely albeit loosely correlated to the degree of parathyroid hormone (PTH) elevation in patients with PHPT [6]. Furthermore, current biochemical indices do not adequately explain the wide spectrum of PHPT disease presentation that includes a clinically distinct subset of patients with a more severe disease phenotype characterized by greater bone loss and fracture burden. The underlying reasons for this well-recognized disparity in clinical presentation remain unknown [7–11].

Despite the extremely variable clinical presentation of the disease, there has not been a significant effort to date to define the mechanisms underlying PHPT phenotypic heterogeneity. Prospective ascertainment of demographic, clinical, biochemical, and histological data in a significant PHPT dataset are required to identify potential contributing factors. However, the paucity and limited scope of previous studies, which have focused

primarily on surgical outcomes, has limited the ability to characterize the population of patients with more severe PHPT [12, 13]. Given this knowledge deficit, our goals were (1) to evaluate relevant clinical data in a large population of unselected patients with established PHPT in order to better understand the phenotypic variability observed in this disease; and (2) to define parathyroid neoplasia cellular behavior functionally in a novel ex vivo platform, as a potential predictor of preoperative disease severity in patients referred for parathyroidectomy.

2.1 Materials and Methods

2.1.1 Parathyroid registry construction

Patients preoperatively diagnosed with PHPT who were referred to Duke University Medical Center for surgical management were eligible for participation and enrolled after providing fully informed consent as described under an IRB-approved protocol (Pro00046210). Pertinent preoperative clinical information was obtained through review of Duke Maestro Care, an EPIC-based electronic health record, as well as outside clinical documents from referring providers. Following surgery, patients were seen within 4 weeks and at 6 months, although the current analyses are focused primarily to preoperative and intraoperative data. The REDCap ™ (Research Electronic Data Capture, Vanderbilt University) System, a secure, web-based application specifically designed to support data capture for research, was selected to create the electronic database. The registry comprises six categories of data collection instruments: Patient demographics, clinical, and biochemical characteristics, and intraoperative, short-term postoperative, and 6-month postoperative laboratory variables. Data accuracy was ensured through scheduled audit and data cleaning where indicated.

2.1.2 Procurement of patient material

All procedures on materials derived from human subjects were reviewed and approved by the Duke University Institutional Review Board (IRB). Parathyroid tumor sections were prepared from surgically resected tissue obtained from patients with PHPT undergoing parathyroidectomy at Duke University Medical Center. Parathyroid tissue identity was established by ex vivo aspiration of the resected tissue with confirmation demonstrated by an off-scale (>5,000 pg/ml) result using the rapid intraoperative PTH assay (Roche Cobas e411 analyzer, iPTH STAT reagent kit, cat. #04892470160, Roche Diagnostics USA), along with serial intraoperative peripheral blood monitoring using the Miami criteria [14] of a >50% decline from preoperative PTH levels within 10 minutes of tumor resection; results were confirmed by postoperative histopathological assessment of the surgical specimen. De-identified parathyroid surgical specimens were provided to the laboratory for immediate harvest and recovery of viable tumor sections.

2.1.3 Tissue sectioning

Viable parathyroid tumor sections were prepared at 300 micron thickness using a Leica VT1000S vibratome as previously described [15].

2.1.4 Calcium EC50 measurements

Calcium responsiveness in viable parathyroid tumor sections was visualized by live-cell calcium flux imaging using the intracellular flux indicator Fluo-4-AM as previously described [15]. Briefly, the tissue slices were loaded with Fluo-4-AM, immobilized in a low melt agarose bed, and then positioned for imaging in a Zeiss 780 multiphoton laser-scanning upright confocal microscope fitted with a 20X water immersion objective lens (20X/1.0 Water W Plan-Apochromat 421452-9800, WD 1.8 mm). The size of the imaging field is set to 600 square microns, an area that typically encompasses several hundred to a thousand or more individual cells. Data acquisition at each calcium concentration point includes at least two randomly selected, non-contiguous image fields vetted for comparable cellular content and density. After a 30 second baseline read interval, parallel tissue sections were stimulated with a series of extracellular calcium concentrations (0.5, 0.75, 1.0, 1.25, 2.0, 3.0, 5.0, and 10.0 mM $CaCl_2$) and CASR signaling activity was monitored by visualizing Fluo-4-AM fluorescent intensity at 5 second intervals over an 11-minute observation period. The test order of calcium concentrations was randomized for each imaging session, avoiding back-to-back repetitions of individual calcium concentration point replicates. For each section, 132 sequential images were recorded. Fluo-4-AM emission was captured using GaAsP high QE 32 channel spectral array detectors and a standard green fluorescence filter cube. Live-cell image stacks with their associated metadata were exported as Zeiss Zen software *lsm* files and analyzed using Fiji, an open-source Image-J based processing package (http://fiji.sc). For quantitation of Fluo-4 live-cell fluorescent intensity, the image stacks were converted into z-projections and overlays were created to align the Hoechst-stained nuclei with the Fluo-4 channel output. The Cell Counter module of ImageJ was employed to determine the total number of nuclei in each image field as a readout of cell number. Fluo-4 threshold fluorescence intensity was adjusted with the 3D Object Counter 2.0 tool using the 6 consecutive pre-stimulation images as a baseline reference for each tissue slice. Maximally responsive cells are defined as those in which the amplitude of the fluorescence signal increases ≥3X over cell-specific pre-stimulation background within 60 seconds of stimulus addition and sustain this plateau (<10% intensity deviation) throughout the post-stimulation observation period [16]. Ionomycin is added to every slice culture specimen as a positive control and the resulting calcium flux is recorded for an additional 1 minute at the end of every observation period. The proportion of responsive cells was determined relative to the total number of cells in each field. The calcium EC50 metric was calculated by plotting the proportion of responsive cells as a function of log calcium concentration and fitting a curve using the standard variable slope, four parameter log (agonist) vs response equation in Prism 6.0 software (Graphpad, San Diego, CA).

2.1.5 Bone Mineral Density Measurements

Dual Energy X-ray Absorptiometry (DXA) determined BMD T scores of the lumbar spine, femoral neck, total hip and one-third radius were obtained preoperatively using Hologic (Hologic Inc., Bedford, MA) or GE-Lunar (Lunar, GE Medical Systems, Madison, WI) densitometers, either within the Duke University Health System (DUHS) or by referring providers. The number of patients who had preoperative DXA studies performed at our institution versus an outside provider were equivalent. DXA scans performed at Duke were analyzed according to ISCD criteria to exclude vertebrae that were inappropriate for analysis

due to artefactual changes. Outside DXA scan images were analyzed when available to exclude scans with excessive vertebral artefactual changes. BMD T scores were based on young normal reference ranges (manufacturer-specific or National Health and Nutrition Examination Survey-based normative data). Where available, DXA images were reviewed to ensure accurate analysis. Lowest T score site was identified for the primary analysis, based on established guidelines on diagnostic assignment of osteoporosis [17].

2.1.6 Statistical Methods

A sample size of 73 patients was required to allow 80% power to detect a Spearman Rank correlation between calcium EC50 and lowest T score of −0.300 at the α=0.10 significance level. This sample size calculation was conducted in PASS 14 Power Analysis and Sample Size software program (NCSS, LLC, Kaysville, UT). Patient data for a total of 237 patients were extracted from the study database on December 1st, 2016. 180 patients (76%) had tissue collected, and 74 (31%) had calcium EC50 collected. BMD data were available for 115 patients. Of the 74 patients who had calcium EC50 collected, 51 had BMD data available. Patient demographic, clinical, biochemical, laboratory, operative, and follow-up characteristics were summarized with N (%) for categorical variables and median (interquartile range) for continuous variables. Creatinine-corrected urine calcium was calculated as urine calcium/(urine creatinine/1000). Albumin-adjusted calcium was calculated as serum calcium+(0.8*(albumin–4.2)). Vitamin 25 OH D insufficiency was defined as <20 ng/mL. Focality was defined as multifocal if more than one gland (tumor) was present, and unifocal otherwise. Lowest BMD T-score was taken from the site with the lowest reported t-score out of all sites measured.

Univariate Spearman Rank correlation was used to estimate the association of calcium EC50 with lowest T score, intact parathyroid hormone (iPTH), and creatinine-corrected urine calcium. Partial Spearman Rank correlation was used to estimate these associations after adjustment for covariates such as gender, vitamin 25 OH D level, age at consent, and body mass index (BMI). Wilcoxon Rank Sum tests were used to test for differences in iPTH and calcium EC50 for patients with vitamin 25 OH D sufficiency vs. insufficiency.

Based on visual inspection, calcium EC50 was segregated into two value groups: <3.0 and ≥3.0 mM. This grouping was validated by applying k-means clustering with only the number of clusters specified as 2 [18]. This algorithm groups observations into homogeneous subsets without knowledge of a splitting value. Application of k-means clustering resulted in the same group indication as was done with visual division (Supplemental Figure 2). iPTH, tumor size, creatinine-corrected urine calcium, lowest t-stage, and focality were summarized and compared between calcium EC50 groups. Wilcoxon Rank sum and Fisher's Exact tests were used to test for differences in continuous and categorical variables, respectively. In order to determine if there was an association between calcium EC50 group and iPTH after adjustment for albumin-adjusted calcium, robust regression was used to calculate an adjusted p-value [19]. With a limited sample size, robust regression allows for more reliable estimates and higher statistical efficiency in the presence of outliers or skewed data. Traditional regression is appropriate and more powerful when the sample size is large and/or the data does not contain outliers or leverage points.

Robust regression can be used in place of traditional regression in any situation, but is exceptionally useful when there is a limited sample size or the data is skewed. This methodology detects observations that have unusual values in the outcome variable, the predictors, or both, and then weights these values based on how they behave in relation to the other data points. It allows for all of the observations to be included in the modeling, while moderating the effect that outliers may have on the resulting estimates.

To determine if the patients that had calcium EC50 collected were representative of all PHPT patients in the registry, a sensitivity analysis was done comparing several clinical variables from these patients with patients who did not have calcium EC50 collected. Patients were divided into two groups: those with calcium EC50 collected (N=74) and those without calcium EC50 collected (N=163) and patient demographic and clinical variables, including age, BMI, race, incidence of pathologic fracture, incidence of peptic ulcer, and number of glands removed, were compared between groups. Continuous variables were compared using the Wilcoxon rank sum test and categorical variables were compared with the Fishers' exact test. Scatter and box plots were used to visualize data relationships. Only patients with available data were included in each analysis, and sample sizes are reported in each table. No adjustments were made for multiple comparisons. All statistical analyses were conducted using SAS version 9.4 (SAS Institute, Cary NC).

3.1 Results

We assembled a comprehensive clinical registry of pre-, peri-, and postoperative patient information from 237 patients undergoing parathyroidectomy for PHPT at our institution and imported these data into a secure, limited-access Redcap database. Of this cohort, 74 subjects had available calcium EC50 data and provided the basis for our analyses. The demographic and clinical characteristics of the study population are shown in Table 1. Pertinent preoperative biochemical characteristics of the cohort are shown in Table 2. Tumors from a subset of the overall cohort were evaluated for biochemical responsiveness, and clinical findings from these patients were reviewed. A sensitivity analysis comparing this cohort of patients with patients who did not have calcium EC50 collected revealed that there were no differences in demographic, clinical, or biochemical characteristics between the two groups. Specifically, age (p=0.57), iPTH (p=0.19), creatinine-corrected calcium (p=0.81), and albumin-adjusted calcium (p=0.86) were all comparable between patients with or without calcium EC50 data.

Using our previously described live-cell imaging method for quantitating calcium responsiveness in viable parathyroid tumor sections, we evaluated the relative extracellular calcium sensitivity threshold in an unselected sequential series of 74 parathyroid tumors obtained from patients undergoing parathyroidectomy for PHPT. Our metric of calcium sensing represents a cumulative population measure based on the responses of several thousand cells per tumor and reflects the proportion of responsive cells in a given tumor across a range of extracellular calcium concentrations [15]. We observed a distribution of calcium responsiveness that separated the tumors into two groups based on their relative sensitivity to calcium challenge. An example of differential flux response in two tumors is shown in Figure 1A. A plot of the relative response rates as a function of log calcium

concentrations reveals that the calcium concentration required to induce a half-maximal response (EC50) is 2.48 mM for Tumor 1 compared to 3.30 mM for Tumor 2 (Figure 1B). Extending this analysis, we measured relative calcium sensitivity in an unselected series of 74 parathyroid tumors resected from patients undergoing parathyroidectomy for PHPT. As shown in Figure 2, the tumors segregated into two nonoverlapping populations based upon calcium EC50. The mean calcium EC50 for the minority group (n = 27) was 2.49 mM [95% confidence interval (CI): 2.43–2.54 mM], consistent with reference normal biochemical activity conferred by the wild type calcium sensing receptor (CASR) when expressed in cultured cells [20, 21]. In contrast, a larger group of tumors (n = 47) exhibited attenuated sensitivity to calcium stimulus, with a mean EC50 value of 3.48 mM [95% CI: 3.41–3.55 mM]. Tumor architecture and histopathological appearance were not predictive of biochemical behavior (Supplemental Figure 1).

Upon observing this bimodal distribution of calcium responsiveness, we queried the clinical registry to determine whether tumor biochemical activity could be associated with clinical indicators of disease severity, especially with respect to measures of bone mineral density. BMD data were available for approximately half of the patients. There was no difference in the distribution of calcium EC50 values among patients with or without BMD data (p=0.67). Age (p=0.57), iPTH (p=0.19), creatinine-corrected calcium (p=0.81), and albumin-adjusted calcium (p=0.86) were all comparable between patients with or without calcium EC50 data. The DXA site with the lowest T score was observed most commonly at the femoral neck (19.4%) and distal one-third radius (19.4%), consistent with the expected more pronounced catabolic effect of PTH excess on cortical bone (Supplemental Table 1). Retrospective analysis of the clinical registry data using Wilcoxon Rank Sum and Fisher's Exact tests suggested that patients whose tumors displayed reduced calcium sensitivity (high EC50) presented with significantly more pronounced radiographic evidence of preoperative BMD deficit. The inverse correlation between T-score and tumor calcium EC50 was maintained after adjustment for gender, vitamin 25 OH D level, age, BMI, and intact PTH level (partial correlation = −0.29, p=0.06, Figure 3). Univariate analysis of calcium EC50 and specific T score sites showed similar inverse relationships (lumbar spine: correlation= −0.45, p=0.002; total hip: −0.36, p=0.02; femoral neck: −0.42, p=0.005). This association was observed for female (correlation = −0.49, p=0.001) but not male patients (p=0.54), although the sample size of the latter was relatively modest. Of the 74 subjects in the two EC50 cohorts, 3 had received bisphosphonate therapy. Exclusion of these three patients did not significantly alter the relationship between calcium EC50 and lowest T-score. As expected, vitamin D insufficiency (25 (OH) D < 20 ng/ml) predicted significantly higher intact PTH levels, with a median of 172.5 pg/ml [Interquartile range: 121.5–241.5] for this group compared to patients with vitamin D sufficiency where the median was 105.0 pg/ml [Interquartile range: 81.0–149.0] (p<0.001). No significant difference between high and low calcium EC50 patients was observed in intact PTH, both unadjusted and corrected for albumin-adjusted serum calcium, or in creatinine-corrected urine calcium (all p's>0.05). The duration of time between when a patient met the clinical definition of PHPT and when that patient underwent parathyroidectomy was not significantly different among low and high EC50 patients (10 months vs 16 months respectively, p=0.1487 by Mann Whitney test). There were no differences in calcium EC50 or BMD for patients with adenomas vs hyperplasia

(Supplemental Table 2). Finally, although there was no significant difference noted in tumor size between tumor calcium response subgroups, high calcium EC50 patients had lower T scores (−2.6 vs. −0.9, $p<0.001$) and were more likely to have multifocal disease than low calcium EC50 patients (29.8 % vs 11.1 %, $p=0.09$) (Table 3).

4.1 Discussion

Despite a clear and pressing clinical need, prognostic and predictive indicators of PHPT disease course and outcome remain elusive. The molecular basis for the disease remains poorly characterized at the mechanistic level, with few biomarkers beyond the parathyroid hormone (PTH) itself [22]. To address these limitations, we developed an ex vivo provocative testing assay for direct functional interrogation of the calcium sensing capacity of parathyroid tumors [15, 16]. Using this new platform, we quantitated the relative responsiveness of human parathyroid tumor tissues to changes in extracellular calcium concentration and then assessed whether evidence of biochemically autonomous tumor behavior was selectively associated with clinical presentation or disease course in patients undergoing parathyroidectomy for PHPT. The principal finding of the current study, that patients whose tumors display attenuated calcium sensitivity are at greater risk of bone density deficit, provides important new mechanistic insight into a potential explanation for diversity in clinical presentation among patients with PHPT. Based on this result, we hypothesize that PHPT may arise through alternative mechanisms dependent either on directly compromised calcium sensing capacity in a causative parathyroid tumor in a subset of patients with more severe disease, or on currently unrecognized tumorextrinsic factors that drive hyperplastic but normative calcium-sensing parathyroid gland expansion in patients with less severe disease. Future studies to delineate the specific molecular events that drive the observed variation in tumor calcium sensing capacity will be essential for the identification and testing of potential biomarkers capable of predicting postoperative bone recovery outcome in patients with PHPT.

Bone loss and fractures are a major source of morbidity in PHPT patients. Support for the concept of linking parathyroid tumor biochemical behavior to BMD maintenance and recovery is based both on historical observations and emerging results from ongoing work. Consistent with the goal of reducing fracture risk, BMD generally improves and fracture risk declines following parathyroidectomy in patients with PHPT [23]. The degree of BMD recovery is generally related to the preoperative severity of hyperparathyroidism as measured by PTH and serum calcium, although postoperative change in BMD can be extremely variable between patients [24–26]. A number of studies indicate that patients with more severe preoperative cortical bone mass loss appear to experience a greater degree of postoperative BMD recovery [7, 8, 27–33]. The fact that attenuated calcium sensing in parathyroid tumors is strongly associated with radiographic evidence of BMD deficit suggests that parathyroid tumors with compromised calcium sensing capacity constitute a tumor-intrinsic, biochemically autonomous disease mechanism that may predict a higher likelihood of post-surgical BMD recovery. If validated, this innovative concept could introduce an important new tool for guiding the management of osteoporotic or osteopenic PHPT patients most at risk of compromised bone mass re-accrual and fragility fracture. This translational risk-stratifying approach would be directly germane as most providers currently

withhold anti-resorptive therapy for at least a year following parathyroidectomy to allow for potential BMD re-accrual. Under the current rubric, a significant subset of patients who are destined to experience clinically insignificant BMD re-accrual may be subject to an unnecessary higher risk of fracture, given the availability of anti-fracture therapies that reduce the risk of fracture within 6–12 months of initiation [34].

Although we observed an inverse association between parathyroid tumor autonomy and preoperative BMD in our population, we did not see a parallel relationship between calcium EC50 and preoperative intact PTH or serum calcium levels (Unadjusted Spearman Correlations: EC50 and iPTH = 0.169, p=0.15; EC50 and serum calcium = −0.125, p=0.29). Coupled with fact that BMD loss is itself not predicted by preoperative PTH or serum calcium, our findings are indicative of a more complex PHPT biological mechanism not fully captured by these two data points alone. We propose that the accelerated bone catabolism observed in a subset of PHPT patients may arise through a multifactorial process driven in part by differences in tumor calcium sensing behaviors in conjunction with additional modifiers of skeletal response to PTH. For example, in patients with end stage renal disease and osteoporosis, renal resistance to the effects of PTH is well established and is possibly due to alterations in osteoprotogerin/RANK ligand production and/or PTH receptor 1 (PTHR1) downregulation [35, 36]. Differences in downstream signal transduction upon PTHR1 activation could also result in an incongruous response to circulating PTH [37, 38]. In support of this latter mechanism, genetic association studies have demonstrated a link between PTHR1 gene polymorphisms and BMD [39, 40]. Taken together, these observations suggest that individual patients with PHPT could experience differential skeletal effects to a given level of PTH. While loss of bone density in PHPT patients is likely a multifactorial process, the newly revealed association between tumor biochemical behavior and BMD strongly suggests that diminished calcium sensitivity in a subset of parathyroid adenomas plays an important role in the more severe bone loss experienced by patients with these tumors.

Strengths of the current study include the creation of a unique registry containing extensive prospective clinical, biochemical and histological characterization of a large patient population with defined PHPT, in addition to the novel functional characterization of live parathyroid tumor cell behavior. Limitations include incomplete ascertainment of bone density and calcium EC50 parameters from the overall study cohort, and the possibility that acquisition of calcium EC50 values may be affected by tumor size. In addition, the retrospective design of the current study imposes a number of limitations arising from its reliance in part on historical data from the patients' clinical records. These limitations include the potential for uncontrolled variation in the generation of bone density metrics from DXA scan readings, and the possible contribution of confounding factors to any observed differences between the respective EC50 groups. We feel that these potential limitations have been adequately addressed in our study. The statistical sensitivity analysis demonstrates that the subset of patients with EC50 data are representative of the overall cohort, with no differences among patients with or without BMD data. Moreover, the inverse correlation between T-score and calcium EC50 is statistically robust and is maintained after adjustment for multiple co-variables. The non-symmetrical distribution of tumors between the high and low calcium EC50 categories could potentially be interpreted as a limitation,

but this difference is more likely reflective of the relative frequency of alternative underlying etiologies of PHPT. Recruitment to the study was sequential without prior knowledge of EC50 status, which was only determined postoperatively. As accrual to the registry remains ongoing and was initiated only in February 2015, the limited availability of follow-up clinical and biochemical data at the current time constrains our ability to confirm the potential translational significance of our findings, in particular the critical question of whether calcium EC50 predicts BMD recovery following parathyroidectomy. With the establishment of our parathyroid registry, we are well positioned to address these important questions in future studies as long-term outcome data become available.

5.1 Conclusions

The bimodal distribution of EC50 values we observed in an unselected series of PHPT patients is consistent with the existence of mechanistically distinct sub-classes of parathyroid tumors. This unanticipated divergence in tumor biochemical behavior suggests that PHPT is not an etiologically monolithic disorder and implies that a distinction between tumor-intrinsic and tumor-extrinsic factors could underlie differences in PHPT disease course, provenance, and outcome. Given that nearly half of patients with PHPT present with reduced BMD [8, 10, 22], prospective stratification of individuals least likely to regain BMD after parathyroidectomy could significantly reduce fractures and associated costs via prompt initiation of anti-fracture therapy. Conversely, those patients likely to re-accrue significant BMD through expectant non-pharmacologic follow-up, the convention applied currently to all patients, could be spared the costs and adverse effects that accompany bisphosphonates and other FDA approved anti-fracture therapies [41, 42]. The demonstration of biochemical heterogeneity in parathyroid tumors may be a first step towards developing molecular evidence-based tools for personalized risk stratification and postoperative management of PHPT patients, and especially those who may be selectively subject to higher skeletal fragility. Currently, the general assumption that BMD will improve in most patients following parathyroidectomy, coupled with expectations of poor tolerability and adherence to anti-fracture therapies, prompts most providers to adopt a conservative approach centered on the anticipation of BMD recovery before initiating medical therapy [43]. Development of a perioperative test that could help predict the potential for insufficient BMD re-accrual based on functional tumor characteristics would help inform this challenging management decision by identifying PHPT patients who may benefit from earlier supportive bisphosphonate therapy, thereby potentially improving skeletal outcomes and reducing fragility fracture risk in patients with PHPT.

Supplementary Material

Refer to Web version on PubMed Central for supplementary material.

Acknowledgments

The authors thank Kristen Lynam, R.N., for her outstanding efforts in clinical data management, informed consent procedures, and other essential tasks required for maintaining full compliance with institutional guidelines for human subjects research.

Funding Sources

This work was supported by funds from the Duke Cancer Institute (J.A.S.), an Enhanced Academics in a Basic Laboratory Environment (ENABLE) award from the Duke Private Diagnostic Clinic (T.J.W.), and by NIH grant 1R21CA192004-02 (J.K. and J.A.S.).

Literature Cited

1. Wermers RA, Khosla S, Atkinson EJ, Achenbach SJ, Oberg AL, Grant CS, et al. Incidence of primary hyperparathyroidism in Rochester, Minnesota, 1993–2001: an update on the changing epidemiology of the disease. J Bone Miner Res. 2006; 21:171–7. [PubMed: 16355286]
2. AACE/AAES Task Force on Primary Hyperparathyroidism. The American Association of Clinical Endocrinologists and the American Association of Endocrine Surgeons position statement on the diagnosis and management of primary hyperparathyroidism. Endocr Pract. 2005; 11:49–54. [PubMed: 16033736]
3. Wu B, Haigh PI, Hwang R, Ituarte PH, Liu IL, Hahn TJ, et al. Underutilization of parathyroidectomy in elderly patients with primary hyperparathyroidism. J Clin Endocrinol Metab. 2010; 95:4324–30. [PubMed: 20610600]
4. Morris LF, Zelada J, Wu B, Hahn TJ, Yeh MW. Parathyroid surgery in the elderly. The oncologist. 2010; 15:1273–84. [PubMed: 21159725]
5. Bilezikian JP, Silverberg SJ. Clinical practice. Asymptomatic primary hyperparathyroidism. N Engl J Med. 2004; 350:1746–51. [PubMed: 15103001]
6. Moosgaard B, Christensen SE, Vestergaard P, Heickendorff L, Christiansen P, Mosekilde L. Vitamin D metabolites and skeletal consequences in primary hyperparathyroidism. Clinical endocrinology. 2008; 68:707–15. [PubMed: 17980013]
7. Brown EM. The pathophysiology of primary hyperparathyroidism. J Bone Miner Res. 2002; 17(Suppl 2):N24–9. [PubMed: 12412774]
8. DeLellis RA, Mazzaglia P, Mangray S. Primary hyperparathyroidism: a current perspective. Archives of pathology & laboratory medicine. 2008; 132:1251–62. [PubMed: 18684024]
9. Duan K, Gomez Hernandez K, Mete O. Clinicopathological correlates of hyperparathyroidism. Journal of clinical pathology. 2015
10. Mazzaglia PJ, Berber E, Kovach A, Milas M, Esselstyn C, Siperstein AE. The changing presentation of hyperparathyroidism over 3 decades. Archives of surgery. 2008; 143:260–6. [PubMed: 18347273]
11. Shah VN, Bhadada SK, Bhansali A, Behera A, Mittal BR, Bhavin V. Influence of age and gender on presentation of symptomatic primary hyperparathyroidism. Journal of postgraduate medicine. 2012; 58:107–11. [PubMed: 22718053]
12. Almquist M, Bergenfelz A, Martensson H, Thier M, Nordenstrom E. Changing biochemical presentation of primary hyperparathyroidism. Langenbecks Arch Surg. 2010; 395:925–8. [PubMed: 20623136]
13. Bergenfelz A, Jansson S, Martensson H, Reihner E, Wallin G, Kristoffersson A, et al. Scandinavian Quality Register for Thyroid and Parathyroid Surgery: audit of surgery for primary hyperparathyroidism. Langenbecks Arch Surg. 2007; 392:445–51. [PubMed: 17103223]
14. Carneiro DM, Solorzano CC, Nader MC, Ramirez M, Irvin GL 3rd. Comparison of intraoperative iPTH assay (QPTH) criteria in guiding parathyroidectomy: which criterion is the most accurate? Surgery. 2003; 134:973–9. discussion 9–81. [PubMed: 14668730]
15. Koh J, Hogue JA, Sosa JA. A Novel Ex Vivo Method for Visualizing Live-Cell Calcium Response Behavior in Intact Human Tumors. PLoS One. 2016; 11:e0161134. [PubMed: 27537691]
16. Koh J, Hogue JA, Wang Y, DiSalvo M, Allbritton NL, Shi Y, et al. Single-cell functional analysis of parathyroid adenomas reveals distinct classes of calcium sensing behaviour in primary hyperparathyroidism. J Cell Mol Med. 2016; 20:351–9. [PubMed: 26638194]
17. http://www.iscd.org/official-positions/2015-iscd-official-positions-adult/.
18. Han, J., Kamber, M. Data mining : concepts and techniques. 3. Burlington, MA: Elsevier; 2011.
19. Yohai VJ. High Breakdown-Point and High Efficiency Robust Estimates for Regression. Ann Statist. 1987; 15:642–56.

20. Nesbit MA, Hannan FM, Howles SA, Babinsky VN, Head RA, Cranston T, et al. Mutations affecting G-protein subunit alpha11 in hypercalcemia and hypocalcemia. N Engl J Med. 2013; 368:2476–86. [PubMed: 23802516]
21. Nesbit MA, Hannan FM, Howles SA, Reed AA, Cranston T, Thakker CE, et al. Mutations in AP2S1 cause familial hypocalciuric hypercalcemia type 3. Nat Genet. 2013; 45:93–7. [PubMed: 23222959]
22. Stang, MT., Carty, SE. Clinical Detection and Treatment of Parathyroid Diseases. In: Hunt, JL., editor. Molecular Pathology of Endocrine Diseases. New York: Springer; 2010. p. 139-48.
23. VanderWalde LH, Liu IL, O'Connell TX, Haigh PI. The effect of parathyroidectomy on bone fracture risk in patients with primary hyperparathyroidism. Archives of surgery. 2006; 141:885–9. discussion 9–91. [PubMed: 16983032]
24. Christiansen P, Steiniche T, Brixen K, Hessov I, Melsen F, Heickendorff L, et al. Primary hyperparathyroidism: whole-body bone mineral density in surgically treated Danish patients: a three-year follow-up study. Bone. 1999; 25:597–602. [PubMed: 10574581]
25. Dy BM, Grant CS, Wermers RA, Kearns AE, Huebner M, Harmsen WS, et al. Changes in bone mineral density after surgical intervention for primary hyperparathyroidism. Surgery. 2012; 152:1051–8. [PubMed: 23040710]
26. Koumakis E, Souberbielle JC, Sarfati E, Meunier M, Maury E, Gallimard E, et al. Bone mineral density evolution after successful parathyroidectomy in patients with normocalcemic primary hyperparathyroidism. J Clin Endocrinol Metab. 2013; 98:3213–20. [PubMed: 23783096]
27. Sharma J, Itum DS, Moss L, Chun-Li C, Weber C. Predictors of bone mineral density improvement in patients undergoing parathyroidectomy for primary hyperparathyroidism. World J Surg. 2014; 38:1268–73. [PubMed: 24744114]
28. Christiansen P, Steiniche T, Brixen K, Hessov I, Melsen F, Heickendorff L, et al. Primary hyperparathyroidism: short-term changes in bone remodeling and bone mineral density following parathyroidectomy. Bone. 1999; 25:237–44. [PubMed: 10456391]
29. Denizot A, Grino M, Oliver C. Surgical management of primary hyperparathyroidism in older adults. Journal of the American Geriatrics Society. 2014; 62:1759–63. [PubMed: 25113865]
30. Jacobs L, Samson MM, Verhaar HJ, Koek HL. Therapeutic challenges in elderly patients with symptomatic hypercalcaemia caused by primary hyperparathyroidism. The Netherlands journal of medicine. 2012; 70:35–8. [PubMed: 22271812]
31. Marcocci C, Bollerslev J, Khan AA, Shoback DM. Medical Management of Primary Hyperparathyroidism: Proceedings of the Fourth International Workshop on the Management of Asymptomatic Primary Hyperparathyroidism. J Clin Endocrinol Metab. 2014 jc20141417.
32. Nakaoka D, Sugimoto T, Kobayashi T, Yamaguchi T, Kobayashi A, Chihara K. Evaluation of changes in bone density and biochemical parameters after parathyroidectomy in primary hyperparathyroidism. Endocrine journal. 2000; 47:231–7. [PubMed: 11036865]
33. Nakaoka D, Sugimoto T, Kobayashi T, Yamaguchi T, Kobayashi A, Chihara K. Prediction of bone mass change after parathyroidectomy in patients with primary hyperparathyroidism. J Clin Endocrinol Metab. 2000; 85:1901–7. [PubMed: 10843172]
34. Black DM, Thompson DE, Bauer DC, Ensrud K, Musliner T, Hochberg MC, et al. Fracture risk reduction with alendronate in women with osteoporosis: the Fracture Intervention Trial. FIT Research Group. J Clin Endocrinol Metab. 2000; 85:4118–24. [PubMed: 11095442]
35. Kazama JJ, Shigematsu T, Yano K, Tsuda E, Miura M, Iwasaki Y, et al. Increased circulating levels of osteoclastogenesis inhibitory factor (osteoprotegerin) in patients with chronic renal failure. Am J Kidney Dis. 2002; 39:525–32. [PubMed: 11877571]
36. Picton ML, Moore PR, Mawer EB, Houghton D, Freemont AJ, Hutchison AJ, et al. Down-regulation of human osteoblast PTH/PTHrP receptor mRNA in end-stage renal failure. Kidney Int. 2000; 58:1440–9. [PubMed: 11012879]
37. Kondo H, Guo J, Bringhurst FR. Cyclic adenosine monophosphate/protein kinase A mediates parathyroid hormone/parathyroid hormone-related protein receptor regulation of osteoclastogenesis and expression of RANKL and osteoprotegerin mRNAs by marrow stromal cells. J Bone Miner Res. 2002; 17:1667–79. [PubMed: 12211438]

38. Park HJ, Baek K, Baek JH, Kim HR. The cooperation of CREB and NFAT is required for PTHrP-induced RANKL expression in mouse osteoblastic cells. J Cell Physiol. 2015; 230:667–79. [PubMed: 25187507]

39. Scillitani A, Jang C, Wong BY, Hendy GN, Cole DE. A functional polymorphism in the PTHR1 promoter region is associated with adult height and BMD measured at the femoral neck in a large cohort of young caucasian women. Hum Genet. 2006; 119:416–21. [PubMed: 16508749]

40. Vilarino-Guell C, Miles LJ, Duncan EL, Ralston SH, Compston JE, Cooper C, et al. PTHR1 polymorphisms influence BMD variation through effects on the growing skeleton. Calcif Tissue Int. 2007; 81:270–8. [PubMed: 17885720]

41. Adler RA, El-Hajj Fuleihan G, Bauer DC, Camacho PM, Clarke BL, Clines GA, et al. Managing Osteoporosis in Patients on Long-Term Bisphosphonate Treatment: Report of a Task Force of the American Society for Bone and Mineral Research. J Bone Miner Res. 2016; 31:16–35. [PubMed: 26350171]

42. Reid IR. Short-term and long-term effects of osteoporosis therapies. Nat Rev Endocrinol. 2015; 11:418–28. [PubMed: 25963272]

43. Sankaran S, Gamble G, Bolland M, Reid IR, Grey A. Skeletal effects of interventions in mild primary hyperparathyroidism: a meta-analysis. J Clin Endocrinol Metab. 2010; 95:1653–62. [PubMed: 20130069]

Highlights

- Parathyroid tumors segregate into two groups with differing calcium sensitivity.
- PHPT patients whose tumors have diminished sensitivity to calcium have lower bone mineral density.
- PHPT disease severity may be influenced by tumor relative biochemical responsiveness to extracellular calcium.

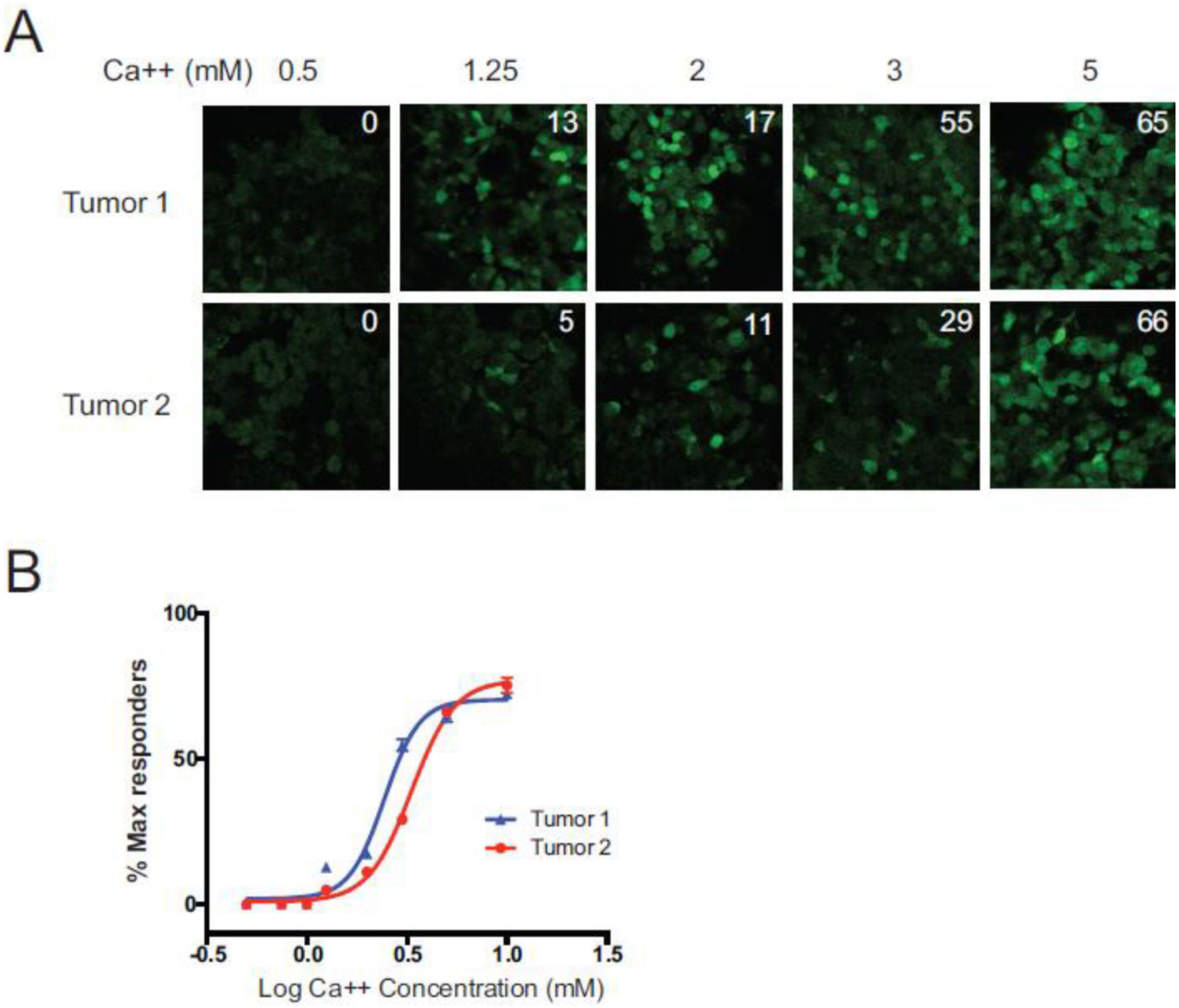

Figure 1.

Differential calcium responsiveness in human parathyroid tumors. (A) Representative images from two different tumors challenged with a series of extracellular calcium concentrations as indicated. Activated Fluo-4-AM fluorescence emission is shown in green, indicative of an intracellular flux response downstream of CASR activation. Images are single frames taken at the same time point (60 seconds after extracellular calcium addition) within the 11-minute observation period for each condition. White numerals indicate the percentage of responsive cells in the total image field at each calcium concentration. (B) Calcium dose-response curves for the tumors shown in (A). The proportion of responsive cells is plotted on the y-axis as a function of log calcium concentration on the x-axis.

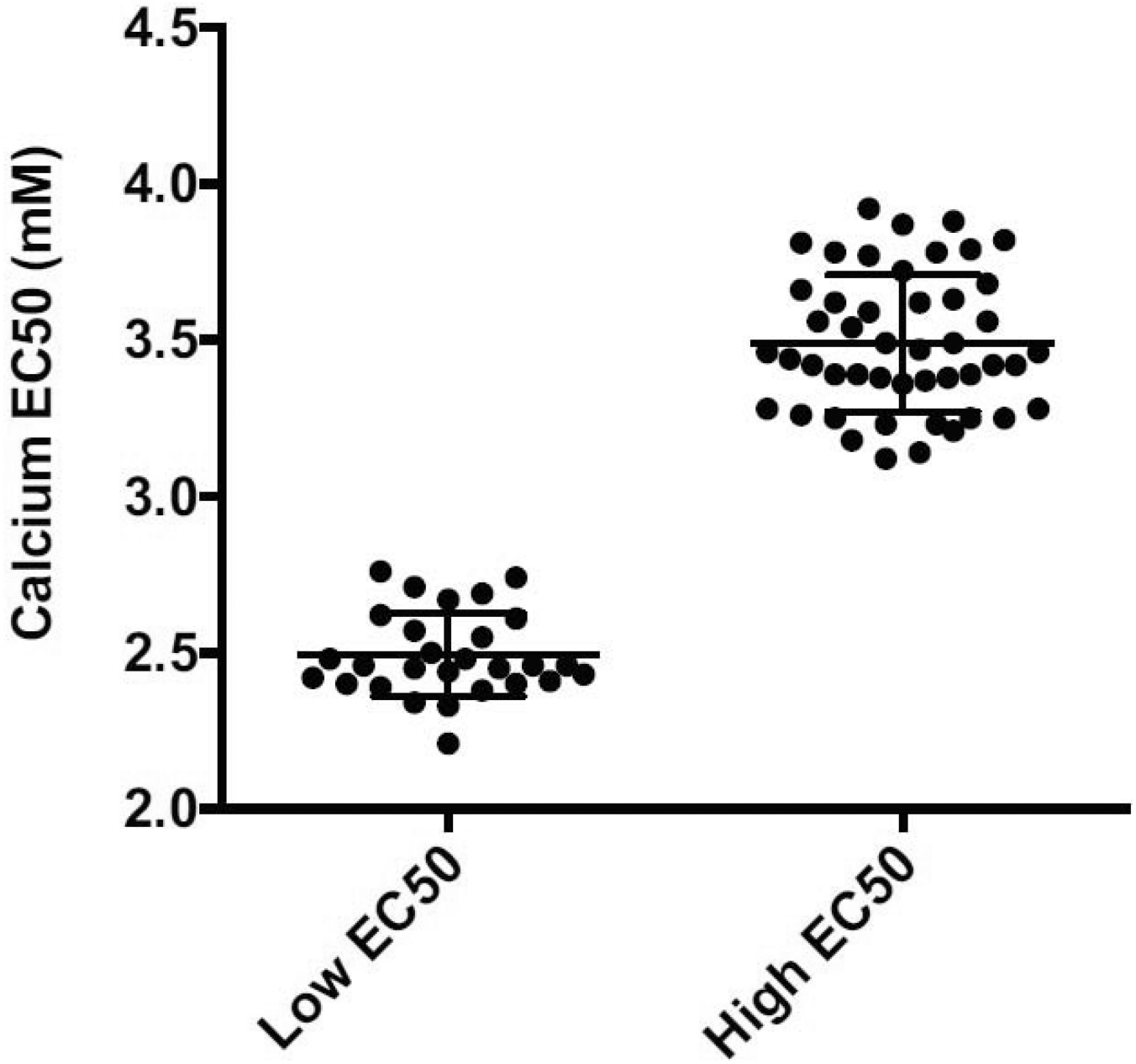

Figure 2.
Bimodal distribution of calcium EC50 in parathyroid tumors. The number of tumors displaying a high (>3.0 mM) or low (<3.0 mM) calcium EC50 is depicted for the tested sample set of 74 specimens.

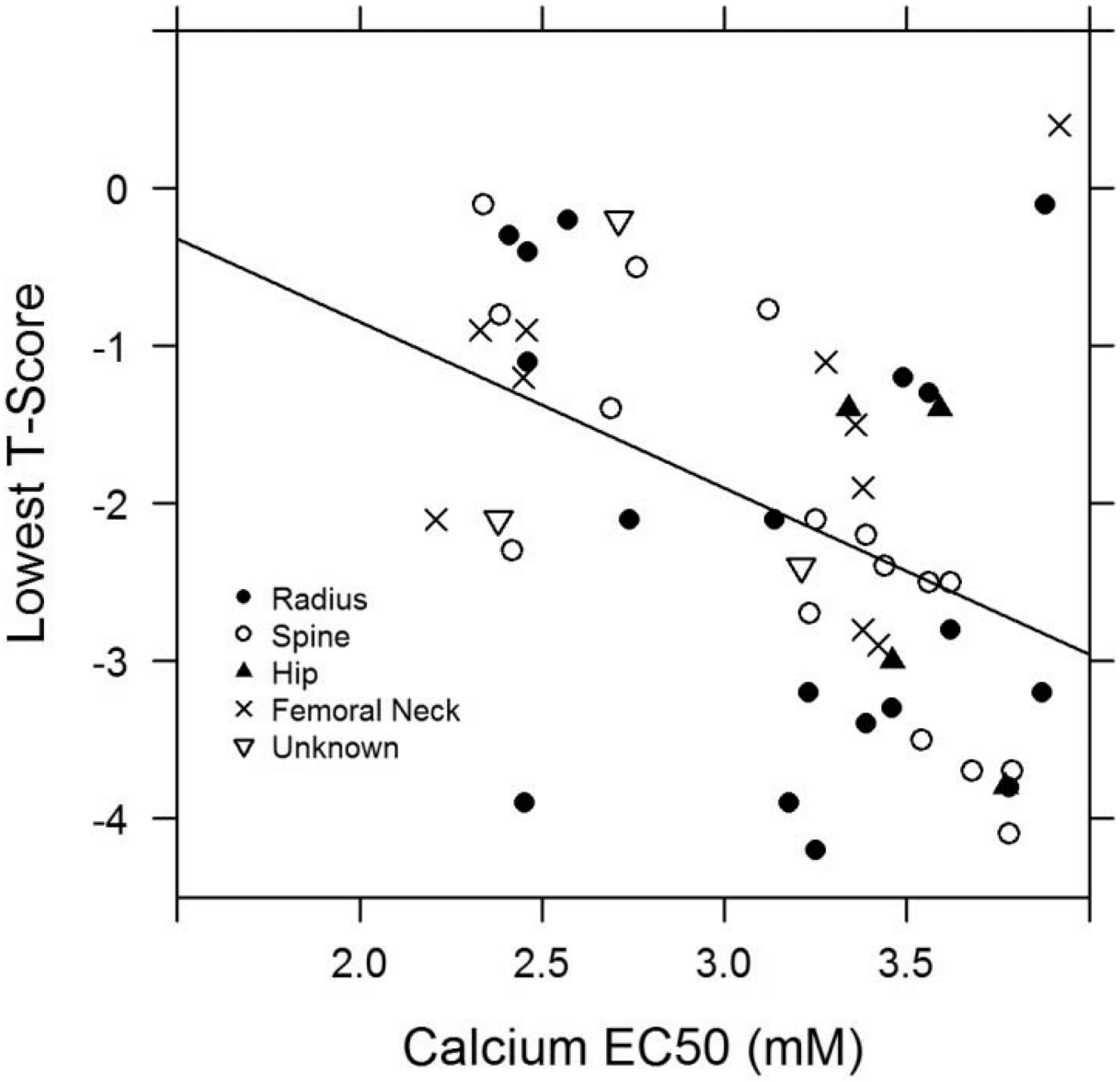

Figure 3.
Correlation between Lowest T-score (y-axis) and calcium EC50 (x-axis). Specific DXA anatomic sites are designated by symbols as described. The fit line represents the approximate unadjusted inverse association.

Table 1

Overall Registry Patient Characteristics (N=237)

	All Patients (N=237)	Patients with CaEC50 (N=74)	Patients without CaEC50 (N=163)
	N (%)	N (%)	N (%)
Demographics			
Age at Consent (Years) – Median (IQR)	62 (52, 70)	64 (52, 70)	61 (51, 69)
Body Mass Index – Median (IQR)	29.17 (25.24, 35.36)	30.65 (25.63, 37.96)	28.57 (24.96, 34.51)
Gender			
Female	181 (76.4%)	60 (81.1%)	121 (74.2%)
Male	56 (23.6%)	14 (18.9%)	42 (25.8%)
Race			
White	176 (74.3%)	54 (73%)	122 (74.8%)
American Indian/Alaska Native	2 (0.8%)	1 (1.4%)	1 (0.6%)
Asian/Native Hawaiian/Pacific Islander	2 (0.8%)	0 (0%)	2 (1.2%)
Black or African American	45 (19%)	15 (20.3%)	30 (18.4%)
Unknown or not reported	12 (5.1%)	4 (5.4%)	8 (4.9%)
Ethnicity			
Hispanic or Latino	15 (6.3%)	6 (8.1%)	9 (5.5%)
Non-Hispanic or Latino	205 (86.5%)	64 (86.5%)	141 (86.5%)
Clinical History			
Nephrolithiasis	53 (22.4%)	20 (27%)	33 (20.2%)
Pathologic Fracture	1 (0.4%)	1 (1.4%)	0 (0%)
Peptic Ulcer Disease	8 (3.4%)	2 (2.7%)	6 (3.7%)
Tumor Histology			
Adenoma	155 (65.4%)	65 (87.8%)	90 (55.2%)
Hyperplasia	21 (8.9%)	8 (10.8%)	13 (8%)
Number of Glands Removed			
1	139 (58.6%)	57 (77%)	82 (50.3%)
2	21 (8.9%)	8 (10.8%)	13 (8%)
3	8 (3.4%)	6 (8.1%)	2 (1.2%)
4	9 (3.8%)	3 (4.1%)	6 (3.7%)

Data are presented as N (%) unless otherwise specified.

Percentages may not add up to 100% due to rounding or missing values. Abbreviations: IQR=Interquartile Range.

Table 2

Preoperative Biochemical Characteristics (N=237)

Biochemical Measure (Normal Range)	All Patients (N=237) Median (IQR)	Patients with CaEC50 (N=74) Median (IQR)	Patients without CaEC50 (N=163) Median (IQR)
Intact Parathyroid Hormone (14–72 pg/ml)	121 (85 – 183)	127.5 (90, 188)	118.5 (81.5 – 174.5)
Serum Calcium (8.7–10.2mg/dl)	10.8 (10.5, 11.3)	10.8 (10.5, 11.3)	10.9 (10.6, 11.3)
Albumin (3.5–4.8g/dl)	4.1 (3.8, 4.3)	4.1 (3.9, 4.3)	4.1 (3.8, 4.3)
Ionized Calcium (1.15–1.32 mM/L)	1.39 (1.33, 1.51)	1.37 (1.28, 1.52)	1.39 (1.34, 1.49)
Albumin-Adjusted Calcium	10.76 (10.36, 11.24)	10.78 (10.42, 11.3)	10.74 (10.32, 11.16)
Serum Creatinine (0.4–1.0 mg/dl)	0.825 (0.7, 1)	0.8 (0.8, 1)	0.85 (0.7, 1)
MDRD calculated GFR (ml/min)	74.99 (61.21, 89.69)	74.09 (61.21, 84.79)	77.395 (61.72, 90.3)
Vitamin 25 D (30–100 ng/ml)	26 (19, 34)	26 (19, 34)	25 (18, 35)
Insufficient (<20 ng/ml) – N (%)	44 (18.6%)	19 (25.7%)	25 (15.3%)
Sufficient (≥20 ng/ml) – N (%)	121 (51.1%)	51 (68.9%)	70 (42.9%)
24 Hour Urine Calcium (50–300 mg)	266 (184, 367)	246 (165, 363)	271 (190, 382)
Creatinine-Corrected Calcium	221.02 (157.32, 294.85)	224.68 (127.27, 303.5)	215.83 (160.4, 284.41)
Lowest T Score *	−2 (−2.7, −1.1)	−2.1 (−3.2, −1.1)	−1.8 (−2.5, −1.15)

Data presented as Median (IQR) unless otherwise specified.

Abbreviations: IQR=Interquartile Range, MDRD=Modification of Diet in Renal Disease, GFR=Glomerular Filtration Rate

*Based on available DXA sites (lumbar spine, femoral neck, total hip or distal radius).

Table 3

Comparison High vs. Low Calcium EC50 groups

	CaEC50 < 3.0 (N=27)	CaEC50 ≥ 3.0 (N=47)	p-value
	Median (IQR)	Median (IQR)	
Calcium EC50	2.457 (2.4, 2.57)	3.46 (3.28, 3.66)	<0.001
Age at Consent (Years)	54 (45, 66)	66 (59, 72)	0.02
BMI	36.73 (30.21, 40.52)	28.68 (24.96, 34.08)	0.004
Gender – N (%)			0.55
Female	23 (85.2%)	37 (78.7%)	
Male	4 (14.8%)	10 (21.3%)	
Lowest T Score	−0.9 (−2.1, −0.4)	−2.6 (−3.4, −1.5)	<0.001
T Score by Site			
Distal Radius	−0.35 (−1.25, 0.25)	−2.45 (−3.35, −1.25)	0.08
Lumbar Spine	0.2 (−0.8, 0.9)	−2.15 (−2.5, −0.3)	0.006
Femoral Neck	−0.7 (−1.2, 0.1)	−1.9 (−2.6, −1.2)	0.002
Total Hip	−0.2 (−1.3, 0.6)	−1.2 (−1.8, −0.4)	0.02
Vitamin 25 D	26.5 (19, 33)	26 (18.5, 35.5)	0.66
Intact Parathyroid Hormone	117 (89, 149)	136 (91, 251)	0.12
Focality			0.09
Multifocal	3 (11.1%)	14 (29.8%)	
Unifocal	24 (88.9%)	33 (70.2%)	